Polymer Chemistry

Accepted Manuscript

This is an *Accepted Manuscript*, which has been through the Royal Society of Chemistry peer review process and has been accepted for publication.

Accepted Manuscripts are published online shortly after acceptance, before technical editing, formatting and proof reading. Using this free service, authors can make their results available to the community, in citable form, before we publish the edited article. We will replace this *Accepted Manuscript* with the edited and formatted *Advance Article* as soon as it is available.

You can find more information about *Accepted Manuscripts* in the Information for Authors.

Please note that technical editing may introduce minor changes to the text and/or graphics, which may alter content. The journal's standard Terms & Conditions and the Ethical guidelines still apply. In no event shall the Royal Society of Chemistry be held responsible for any errors or omissions in this *Accepted Manuscript* or any consequences arising from the use of any information it contains.

ROYAL SOCIETY OF CHEMISTRY

www.rsc.org/polymers

Polymer Chemistry

ARTICLE

The Comparison of N-type Copolymers Based on Cyclopentadithiophene and Naphthalene Diimide/Perylene Diimides for All-Polymer Solar Cells Application

Received 00th January 20xx,
Accepted 00th January 20xx

DOI: 10.1039/x0xx00000x

www.rsc.org/

Bo Xiao,[a] Guodong Ding,[a] Zhan'ao Tan,[b]* and Erjun Zhou [ac]*

All-polymer solar cells (PSCs), using naphthalene diimide (NDI)- or perylene diimide (PDI)-based polymers as electron acceptor have been intensively investigated in recent years. Nevertheless, the lack of comprehensive comparison studies of NDI- and PDI-based polymers have limited the further development of novel acceptor polymers. Here, we conduct a comparative study of two solution-processable cyclopenta[2,1-b:3,4-b']dithiophene (CPDT)-based n-type copolymers, PCPDT-NDI and PCPDT-PDI on the optical, electrochemical and photovoltaic properties. Although PCPDT-NDI has better near-infrared (850-1100 nm) light absorption and crystalline properties, the photovoltaic performance is disappointing mainly due to the poor miscibility with PTB7 donor polymer and inferior film quality. On the contrary, PCPDT-PDI exhibits much better photovoltaic performance with power conversion efficiency of 2.13% by using 1-chloronaphthalene (CN) as additive to obtain good film morphology and improve the electron mobility. The comprehensive comparison of PDI and NDI-based polymers will help to understand the relationship of structure-property-performance and contribute to further development of novel rylene diimide-containing n-type polymers.

Introduction

All-polymer solar cells (all-PSCs) composed of both polymer donor and polymer acceptor have attracted a great deal of attention due to the potential advantages over conventional fullerene-based solar cells: (1) complementary absorption spectra of both polymers for higher short-circuit current (J_{SC}); (2) readily tunable molecular orbital levels for effective charge transfer and higher open circuit voltage (V_{OC}); and (3) the flexibility in controlling solution viscosity and enhanced mechanical/thermal properties for roll-to-roll large area fabrication.[1-4] Although the V_{OC} of all-PSCs could be easily modulated and over 1.0 V has been realized, the overall performance still lags far behind polymer/fullerene bulk heterojunction systems mainly due to the low J_{SC} and fill factor.[5, 6] The limited efficiency mainly comes from the scarcity of excellent acceptor polymers, and thus, developing of solution-processable n-type polymer semiconductors with suitable energy level, wide absorption band, high electron affinity and mobility, remains necessary.[7-11]

So far, two kinds of rylene diimides, including perylene diimide (PDI), naphthalene diimide (NDI), are the most effective building blocks to construct n-type polymer acceptors owing to their excellent chemical and thermal stability, high electron affinities, and remarkable electron-transporting properties. The development of PDI-based polymers for all-PSCs application was earlier than NDI-based polymers. In 2007, Zhan et.al reported the first PDI-based polymer, PDI-dithienothiophene copolymer, which exhibits broad absorption spectrum, high electron mobility of 0.013 $cm^2V^{-1}s^{-1}$ and PCE of over 1% using a polythiophene derivative as donor.[12] After modulation of the chemical structures of the corresponding donor and acceptor polymers, Zhan et al improve the PCE to 1.48%.[7, 13] In 2011, we reported all-PSCs based on six kinds of PDI-based polymers, and the best PCE of 2.23% was achieved by optimizing the solvent.[14] In 2014, Zhan et al utilized binary additives, DIO and PDI-2DTT, and successfully boosted the PCE of all-PSCs based on PBDTTT-C-T:PPDIDTT combination up to 3.45% due to the suitable phase separation and balanced charge transport.[15] In 2013, Zhao et al fabricated inverted all-PSCs with PCE of 2.17% by employing the first 1,7-regioregular PDI-dithiophene copolymer as acceptor and P3HT as donor.[16] In 2014, they enhanced all-PSCs with PCE beyond 4.4%, the highest value for PDI-based polymers, by side-chain engineering of low band gap donor polymers.[17]

On the other hand, the development of solution-processable NDI-based polymer started in 2009, when Facchetti et al reported an excellent electron-accepting polymer P(NDI2OD-T2) with the electron mobility up to 0.85 $cm^2V^{-1}s^{-1}$.[18] However, in the early stage, P(NDI2OD-T2) exhibited disappointing photovoltaic performance. Using classic poly(3-hexylthiophene) (P3HT) as donor, PCE of only 0.2% was achieved by Sirringhaus et al. and Frechet et al.[9, 19] In the same year, Loi et al obtained high fill factor and improved PCE of 0.62% for P3HT:P(NDI2OD-T2) combination by optimizing the photoactive layer morphology.[20] By comparing P3HT:F8TBT with

[a] CAS Key Laboratory of Nanosystem and Hierarchical Fabrication, National Center for Nanoscience and Technology, Beijing, 100190, P. R. China. E-mail: zhouej@nanoctr.cn
[b] Beijing Key Laboratory of Novel Thin Film Solar Cells, School of Renewable Energy, North China Electric Power University, Beijing 102206, P. R. China. E-mail: tanzhanao@ncepu.edu.cn
[c] Yangtze River Delta Academy of Nanotechnology and Industry Development Research, Jiaxing, Zhejiang Province, 314000, P. R. China.

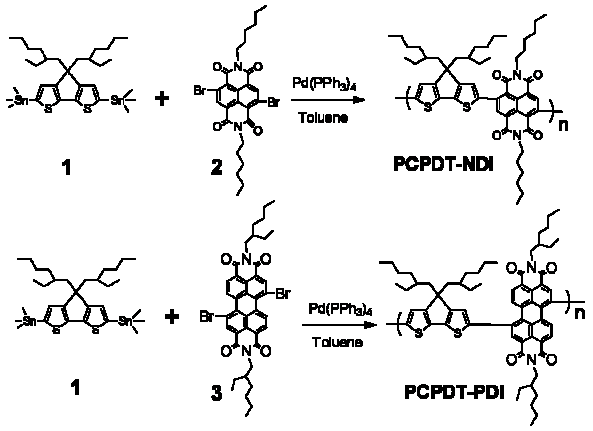

Scheme 1 Synthetic routes of PCPDT-NDI and PCPDT-PDI.

P3HT:P(NDI2OD-T2) device performance, it was found that the large domains driven by crystallization in P3HT:P(NDI2OD-T2) blends is the dominating factor that hampers the device performance.[21] In 2012, the PCE of all-PSCs comprising P3HT and P(NDI2OD-T2) was increased up to 1.4% by using suitable solvent to suppress the preaggregation of naphthalene copolymers.[22] After that, many non-P3HT donor polymers were combined with P(NDI2OD-T2) and photovoltaic performance was greatly improved to 4.1% (PTQ1),[23] 4.35% (PTP8),[24] 4.5% (PTB7-Th),[25] 4.1% (BSF4),[6] 5.03% (PPDT2FBT),[26] 5% (NT),[27] and 5.73% (PBDTTT-EF-T),[28] respectively. Meanwhile, many novel NDI-based polymers were also designed and synthesized. In 2012, we synthesized an NDI-fluorene copolymer and a PCE of 1.6% was achieved by using DIO as additive,[29] and the PCE could be improved to 3.6% by developing an NDI-carbozole copolymer.[30] In 2013, Jenekhe et al synthesized NDI-selenophene copolymer acceptor PNDIS-HD and PCE of 3.3% was achieved by using PSEHTT donor,[31] which could be further improved to 4.8% by solution processing from a co-solvent.[32] In 2014, Kim et al demonstrated an NDI-thiophene copolymer PNDIT-HD as an effective acceptor with 6% PCE benefiting from the face-on crystalline orientation rather than analogous PNDIT-OD and PNDIT-DT with different alkyl side chains.[33] Recently, A fluorinated n-type polymer P(NDIDT-FT2) can be utilized as an efficient electron acceptor in PBDTT-TT-F:P(NDIDT-FT2) system, resulting in a very high PCE of 6.7% without any solvent additive.[34] Very recently, a new PCE record of 7.7% was achieved by employing suitable acceptor polymer of PNDIS-HD and donor polymer of PBDTT-FTTE.[35]

As mentioned above, it could be found that NDI-based all-PSCs exhibited PCE as high as 7.7%, which is superior than that of PDI-based all-PSCs. In these reported copolymers, NDI-based copolymers, in general, exhibit better crystallinity and higher electron mobility than that of PDI-based polymers. However, the detailed comparison of two kinds of polymers in one report was limited,[36] and it is also vital to investigate the different properties of PDI and NDI-based polymers and to understand the relationship of structure-property-performance.[37, 38] Here, we choose a planar building block cyclopenta[1,2-b:5,4-b']dithiophene (CPDT) to copolymerize with NDI and PDI moiety, respectively, and systematically investigate the different properties and dominating factors for photovoltaic performance by choosing excellent p-type polymer PTB7 as donor.[39-43] The synthetic routes and chemical structures of these two n-type semiconducting polymers, namely PCPDT-NDI and PCPDT-PDI, were shown in Scheme 1.

Experimental

Synthesis of polymers

All chemicals were purchased from Alfa, Aldrich, TCI or Wako and used without any treatment and further purification. The copolymers PCPDT-NDI and PCPDT-PDI were synthesized according to the following procedures:

Poly{4,4-bis(2-ethylhexyl)-cyclopenta[2,1-b:3,4-b']dithiophene-2,6-diyl-*alt*-N,N'-dihexyl-1,4,5,8-naphthalene diimide-2,6-diyl} (PCPDT-NDI). Monomer 1 (473mg, 0.65 mmol), monomer 2 (385 mg, 0.65 mmol) and dry toluene (10 mL) were added to a 50 mL double-neck round bottom flask. The reaction container was purged with N_2 for 30 min to remove O_2. $Pd(PPh_3)_4$ (3%, 23 mg) was added, and heated up to 110 °C. The solution was stirred at 110 °C for 48 h. The dark blue sticky solution was cooled down to room temperature and poured into methanol and the precipitate was filtered and washed with methanol and hexane in a soxhlet extractor to remove the oligomers and catalyst residue. Finally, the polymer was extracted with chloroform. The solution was condensed by evaporation and precipitated into methanol, and the polymer was collected as a dark blue solid. Yield: 270 mg (52%). ^{1}H NMR ($CDCl_3$, 400MHz): ^{1}H NMR ($CDCl_3$, 400 MHz): δ(ppm) 8.8 (br, 2H), 7.0 (br, 2H), 4.0 (br, 4H), 2.0-0.7 (br, 56H). M_n = 12.4 kg mol^{-1}; polydispersity = 1.6.

Poly{4,4-bis(2-ethylhexyl)-cyclopenta[2,1-b:3,4-b']dithiophene-2,6-diyl-*alt*-N,N'-di(2-ethylhexyl)-3,4,9,10-perylene diimide-1,7-diyl} (PCPDT-PDI). A procedure similar to the synthesis of **PCPDT-NDI** was adopted by using monomer **1** (728 mg, 1.0 mmol), monomer **3** (772.6 mg, 1.0 mmol), dry toluene (20 mL) and $Pd(PPh_3)_4$ (3%, 35 mg). The polymer was collected as a dark blue solid. Yield: 610 mg (60%). ^{1}H NMR ($CDCl_3$, 400MHz): δ(ppm) 8.7-8.0 (m, 6H), 7.1(br, 2H), 4.1 (br, 4H), 1.9-0.6 (br, 64H). M_n = 11.8 kg mol^{-1}; polydispersity = 1.9.

Characterization

^{1}H NMR (400 MHz) spectra were measured using a JEOL Alpha FT-NMR spectrometer equipped with an Oxford superconducting magnet system. The molecular weights of polymers were estimated by high temperature gel permeation chromatography at 160 ° C using 1,2,4-tricholorobenzene as the solvent and polystyrene as a standard. Absorption spectra were measured using a JASCO V-660 spectrometer. The concentration of the polymers in $CHCl_3$ solutions was 5×10^{-3} g L^{-1} and the films were spin-coated from $CHCl_3$ solutions (5 g L^{-1}). Cyclic voltammograms (CVs) were recorded on an HSV-100 (Hokuto Denkou) potentiostat. A Pt plate coated with a thin polymer film was used as the working electrode. A Pt wire and an Ag/Ag^+ (0.01 M of $AgNO_3$ in acetonitrile) electrode were used as the counter and reference electrodes (calibrated against Fc/Fc^+), respectively. Atomic force microscopy (AFM) was conducted in tapping mode with a 5400 scanning probe microscope (Agilent Technologies). XRD patterns were recorded on a Rigaku SmartLab X-ray diffractometer. The films were prepared by spin-coating chlorobenzene solutions of the polymers (10 g L^{-1}) on Si substrates

and thermally annealed at 80 °C for 30 min.

Fabrication and characterization of polymer solar cells

PSCs were fabricated with the conventional sandwich structure through several steps. ITO-coated glass substrates were cleaned by ultrasonication sequentially in detergent, water, acetone and 2-propanol. After drying the substrate, PEDOT:PSS (Baytron P) was spin-coated (4000 rpm, 30 s) on ITO. The film was dried at 150 °C under N_2 atmosphere for 5 min. After cooling the substrate, a blend solution of PTB7 and PCPDT-NDI (or PCPDT-PDI) with the total concentration of 20 g L^{-1} was spin-coated. The substrate was annealed at 80 °C for 30 min inside a nitrogen-filled glove box to dry the solvent completely, after which a Ca/Al (20 nm/60 nm) electrode was evaporated onto the substrate under high vacuum (<10^{-4} Pa) in an evaporation chamber (ALS Technology, H-2807 vacuum evaporation system with E-100 load lock). Photovoltaic cells without protective encapsulation were subsequently tested in air under simulated AM1.5 solar irradiation (100 mW cm^{-2}, Peccell Technologies, PCE-L11). The light intensity was adjusted by using a standard silicon solar cell with an optical filter (Bunkou Keiki, BS520). The current-voltage characteristics of the photovoltaic cells were measured using a Keithley 2400 I-V measurement system. The external quantum efficiency (EQE) of the devices was measured on a Hypermonolight System (Bunkou Keiki, SM-250F). The configuration of the shadow mask afforded eight independent devices on each substrate, with an active layer of ~0.21 cm^2 (3 mm × ~7 mm) for each device. The effective area of the PSCs was defined using a metal photomask (2 mm × 3 mm) during irradiation with simulated solar light.

Hole and electron mobility measurement by space-charge-limited current (SCLC) method

Hole- and electron-only devices were fabricated by using the device structures of glass/ITO/PEDOT:PSS(30 nm)/active layer/MoO_3(5 nm)/Au(60 nm) and glass/ Al(60 nm)/active layer/Al(60 nm), respectively. The active layers were spin-coated from chloroform solution with the total concentration of 15 mg mL^{-1}. Both hole and electron mobilities were calculated with the Mott–Gurney equation in the SCLC region (slope = 2):

$$J = \frac{9}{8}\varepsilon_0\varepsilon_r\mu\frac{V^2}{L^3}$$

where ε_0 is the permittivity of the vacuum, ε_r is the dielectric constant of the polymer (assumed to 3), L is the thickness of the polymer layer.

Results and discussion

Synthesis and characterization

Monomer **2** is a pure 2,6-dibromo compound but monomer **3** is a mixture of 1,7 and 1,6 regio-isomers with the ratio of about 85:15. Due to the difficulty to get pristine 1,7 regio-isomer, in this paper, we did not investigate the effect of 1,6-regio isomers and the mixture 3 is simplified as 1,7-isomer. [44] The monomers 4,4-Bis(2-ethylhexyl)-2,6-bis(trimethylstannyl)-cyclopenta [2,1-b:3,4-b']dithiophene (monomer **1**), monomer **2** and monomer **3** were synthesized according to the known procedures in the literatures.[14, 29, 30] The new n-type copolymers PCPDT-NDI and PCPDT-PDI were synthesized by Stille coupling copolymerization of monomer **1** with monomer **2** and monomer **3**, respectively. The number averaged molecular weight (M_n) of the PCPDT-NDI and PCPDT-PDI were 12.4 and 11.8 kg mol^{-1} with a polydispersity index (PDI) of 1.6 and 1.9, respectively, which were measured by gel permeation chromatography (GPC) at 160 °C using 1,2,4-tricholorobenzene as a solvent. The polymers have good solubility in common organic solvents such as CF , chlorobenzene (CB) and dichlorobenzene (DCB).

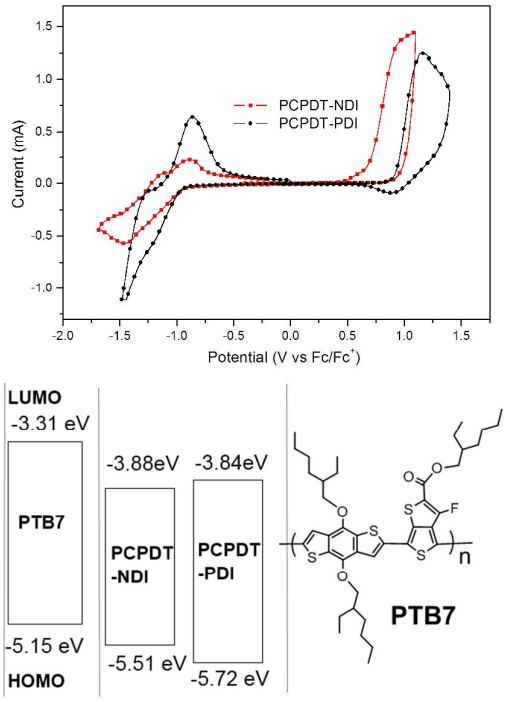

Fig. 1 Cyclic voltammogram of PCPDT-NDI and PCPDT-PDI films on a platinum plate, together with the energy levels and the chemical structure of PTB7.

Electrochemical properties

The lowest unoccupied molecular orbital (LUMO) and highest occupied molecular orbital (HOMO) energy levels of PCPDT-NDI and PCPDT-PDI were measured by cyclic voltammetry (CV), and the voltammograms were shown in Fig. 1, together with the energy levels and structure of PTB7. The electrochemical band-gaps of PCPDT-NDI and PCPDT-PDI are 1.63 eV and 1.88 eV, respectively, which will contribute to efficient absorption of solar spectra. The lower band gap of PCPDT-NDI than PCPDT-PDI might come from more delocalized π-conjugating along the polymer backbone. PTB7 has energy levels LUMO (-3.31 eV) and HOMO (-5.15 eV),[45-47] and was utilized as donor polymer for solar cell application. The LUMO offsets of PTB7:PCPDT-NDI and PTB7:PCPDT-PDI are estimated to be 0.57 eV and 0.53 eV, respectively, which would provide large enough driving force for efficient charge separation without too much energy loss.[48] Additionally, the energy offsets of LUMO(acceptor)-HOMO(donor) are calculated to be 1.27 eV and

1.31 eV, which could reduce the charge transfer states geminate recombination at the donor/acceptor interface.

Optical properties

UV-vis absorption was performed to detect the absorption spectra

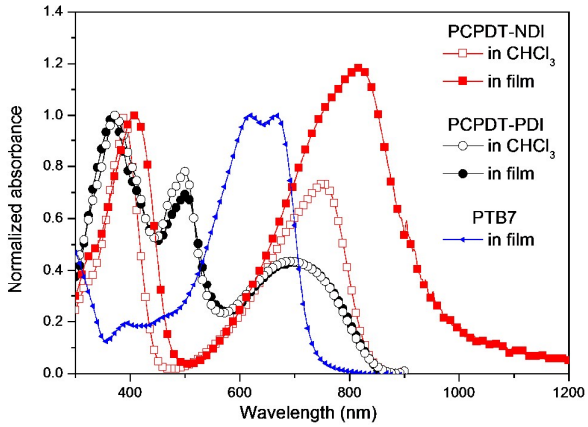

Fig. 2 UV-vis absorption spectra of PCPDT-NDI and PCPDT-PDI in $CHCl_3$ solution and in film on quartz plates, PTB7 in film on quartz plates.

of the donor and acceptor matching with the solar spectrum in the visible and near-IR region. Fig. 1 displays the absorption spectra of PCPDT-NDI and PCPDT-PDI in $CHCl_3$ solution and in film on quartz plates, together with the film absorption of PTB7 donor polymer. The polymer PCPDT-NDI film shows typical NDI-based polymers absorption with two distinctive bands at 300-450 nm and 600-1000 nm, which are assigned to n-π* and π-π* transition and intramolecular charge transfer band, respectively.[32, 49] The normalized absorption spectrum of PCPDT-PDI film shows continuous absorption at the region of 300-900 nm with absorption maxima at 360 nm, 500 nm and 700 nm, which is similar to that of analogous PDTP-PDI polymer.[14] The PCPDT-NDI film shows a broader absorption region extending up to 1000 nm than PCPDT-PDI with absorption edge at 850 nm, which implies larger absorption of photon. Compared with each solution absorption spectrum, PCPDT-NDI shows red-shifted by 16 nm (@??nm) and 65 nm (@??nm) possible due to the intermolecular interactions in the solid state, while PCPDT-PDI has similar spectra, which indicates that PCPDT-NDI has smaller steric hindrance than PCPDT-PDI to ensure forming ordered structure during the spin-coating process. Moreover, the absorption of PTB7 is at the region of 400-750 nm, which can complement the absorption of PCPDT-NDI and PCPDT-PDI to furthest utilize sunlight with the maximum photon flux at 600-800 nm.

X-ray diffraction analysis

X-ray diffraction (XRD) measurements were carried out to understand the crystalline structures and molecular orientations of PCPDT-NDI and PCPDT-PDI in solid state. The films were spin-coated

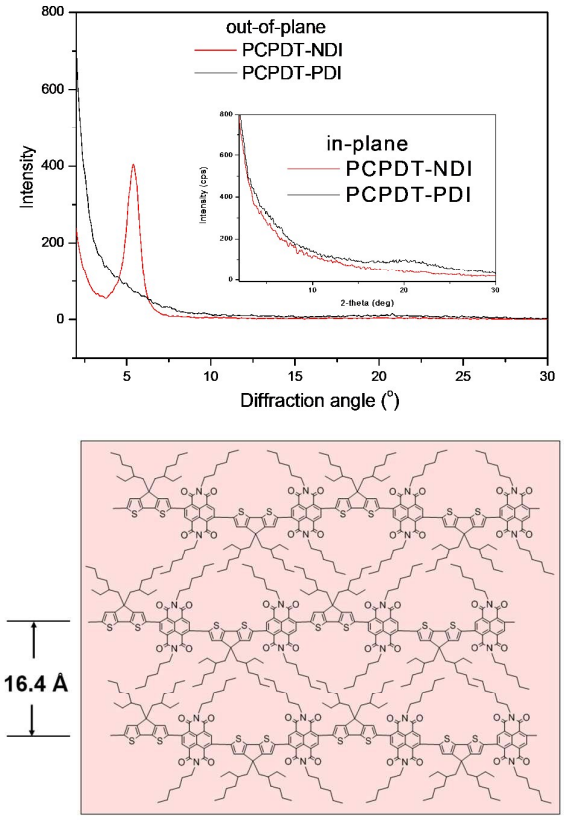

Fig. 3 XRD patterns of PCPDT-NDI and PCPDT-PDI thin solid films along the out-of-plane and in-plane axes and a schematic representation of the possible packing of PCPDT-NDI in the thin solid film.

from a CB solution on Si/SiO_2 substrates and then thermally annealed at 100 °C for 10 min. As shown in Fig. 3, PCPDT-NDI shows one strong diffraction peak at 2θ = 5.4° in the out-of-plane profile, from which the interlayer stacking distance is calculated to be 1.64 nm as shown in Fig. 3b). However, there is no clear peak in that of PCPDT-PDI film, indicating that PCPDT-PDI exhibits amorphous structures in the film, which might result from the relative larger PDI moiety disturbing the planarity of the backbones. For the in-plane XRD curves, both PCPDT-NDI and PCPDT-PDI have no clear peak, although one broad and weak peak at 2θ = 20° corresponding to the π–π stacking is obtained in PCPDT-PDI diffraction curves. Therefore, we can conclude that PCPDT-NDI has more ordered structure in the film.

Photovoltaic properties

Bulk heterojunction (BHJ) all-polymer solar cells (all-PSCs) based on PTB7:PCPDT-NDI and PTB7:PCPDT-PDI combinations were fabricated with a conventional sandwich structure of ITO/PEDOT:PSS/active layer/Ca/Al to investigate their photovoltaic properties. The performance of PSCs was optimized by changing the weight ratio of donor and acceptor as wll as the thickness of the blend film. The weight ratio of 1:1 and the thicknesses of 80-90 nm for both PTB7:PCPDT-NDI and PTB7:PCPDT-PDI systems gave the

best photovoltaic performance. The optimal current density-voltage (*J-V*) curves under simulated solar light illumination (AM 1.5, 100 mW cm^{-2}) are given in Fig. 4 and the corresponding photovoltaic parameters are summarized in Table 1, where different solvents (CB, DCB, CF) without and with additive CN were used to spin-coat the active layers.

The PTB7:PCPDT-NDI devices fabricated by CB and DCB solvents yielded relatively low PCE of 0.87%. When CF was used as solvent, the best PCE reached up to 1.12% with V_{OC} = 0.74 V, J_{SC} = 3.85 mA cm^{-2} and FF = 0.39. Upon addition of 1.0 v% solvent additive CN into CF solvent, the PCE largely decreased to 0.76% with decreasing of J_{SC} = 2.57 mA cm^{-2}. In the case of PTB7:PCPDT-PDI device, CF solvent exhibited higher PCE of 1.38%, slightly higher than CB solvent. However, the addition of 1.0 v% CN into CF could improve the PCE up to 2.13% from 1.38%, which is different with PTB7:PCPDT-NDI. The V_{OC} slightly decreased from 0.74 V to 0.70 V, J_{SC} largely increased from 4.74 mA cm^{-2} to 7.25 mA cm^{-2}, and FF slightly increased from 0.39 to 0.42. This result indicated that the additive CN mainly affect the J_{SC} of the devices. After further increasing the concentration of additive CN to 3 v%, the PCE decreased to 1.46% with lower J_{SC} of 4.85 mA cm^{-2}. Therefore, 1 v% of additive CN in the solvent is the optimal condition for high photovoltaic performance in PTB7:PCPDT-PDI devices. Moreover, the efficiencies were significantly higher than previously reported PSBTBT:PCPDT-PDI device with an inferior PCE of 0.43%, indicating that PTB7 was an effective electron donor to combine with PDI-based copolymers.[50] The experimental observed V_{OC} values of PCPDT-PDI are similar to that of PCPDT-NDI, which is consistent with the energy differences between HOMO(D) and LUMO(A).[51] The J_{SC} of PCPDT-PDI device is much higher than PCPDT-NDI, although PCPDT-NDI has a broader absorption than PCPDT-PDI, which might come from the more ideal morphology in PTB7:PCPDT-PDI system. It has been reported that additive could affect the aggregation of active layer.[52] Therefore, we used atomic force microscopy (AFM) technique to investigate the morphology of the blend films. The height images of PTB7:PCPDT-NDI and PTB7:PCPDT-PDI films are shown in Fig. 5. For the films of PTB7:PCPDT-NDI, CB and DCB films show large aggregation domain, while CF film shows better phase separation. Upon addition of 1.0 v% CN into CF, the film shows large aggreation again. The uniform film is benificial to forming charge transfer state at the donor/acceptor interface, while the aggregation phase is favor of free charge carrier transport in the continuous pathway.

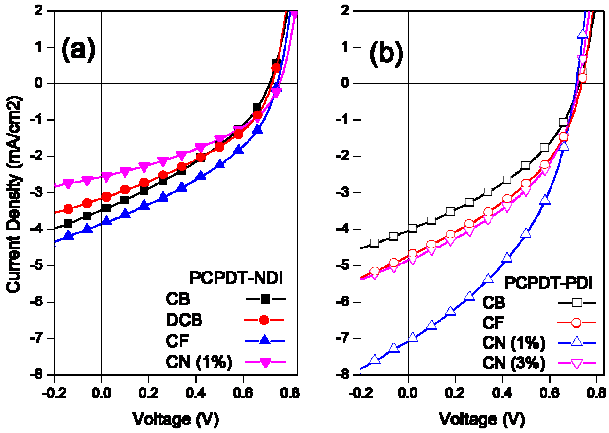

Fig. 4 *J-V* curves of photovoltaic devices based on (a) **PTB7**: **PCPDT-NDI** and (b) **PTB7**: **PCPDT-PDI**, under the illumination of AM 1.5, 100 mW/cm^2.

Table 1 Photovoltaic performances of all-PSCs based on **PTB7**:**PCPDT-NDI** and **PTB7**:**PCPDT-PDI**

Active layer	Solvent	V_{OC} (V)	J_{SC} (mA cm^{-2})	FF	PCE
PTB7:**PCPDT-NDI**	CB	0.72	3.74	0.35	0.87%
	DCB	0.72	3.16	0.38	0.87%
	CF	**0.74**	**3.85**	**0.39**	**1.12%**
	CF:CN (99:1 v/v)	0.76	2.57	0.39	0.76%
PTB7:**PCPDT-PDI**	CB	0.72	4.05	0.39	1.14%
	CF	0.74	4.74	0.39	1.38%
	CF:CN (99:1 v/v)	**0.70**	**7.25**	**0.42**	**2.13%**
	CF:CN (97:3 v/v)	0.72	4.85	0.42	1.46%

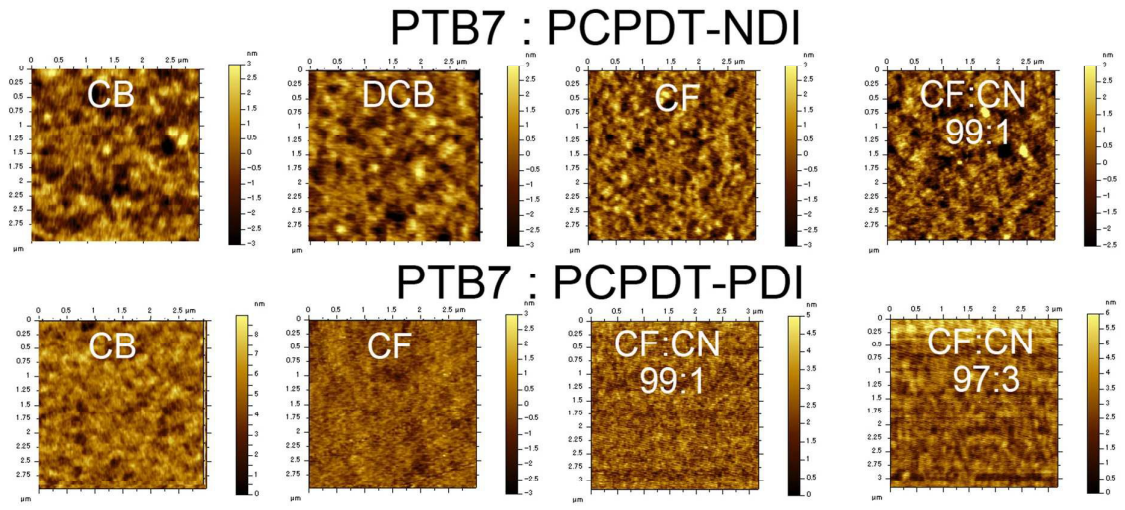

Fig. 5 AFM height images of **PTB7**:**PCPDT-NDI** and **PTB7**:**PCPDT-PDI** films spin-coated from CF with different amount of CN in the solutions.

For PTB7:PCPDT-PDI films, CF resulted in a much more smooth film surface than CB. Upon addition of 1.0 v% CN to CF, better phase separation could be obtained with crystallization phase. However, 3.0 v% CN induced large aggregated grains. Comparing the films spin-coated from CF, PTB7:PCPDT-NDI exhibited large aggregation grains, while PTB7:PCPDT-PDI was uniform and smooth, which could be ascribed to the strong aggregation ability and ordered structure of PCPDT-NDI. Moreover, the effect of additive CN on the aggregation of donor polymer PTB7 cannot be neglected, which will be further proved below. Consequently, the additive CN has large effect on the morphology of blend films containing different polymers, which finally result in difference photovoltaic efficiency. Furthermore, after choosing other promising p-type polymers with good miscibility with PCPDT-NDI, the photovoltaic performance could be improved.[53-55]

Charge Mobility

As discussed above, PTB7:PCPDT-PDI device fabricated with mixture solvent CF:CN (99:1, v/v) shows best PCE with relatively higher J_{SC} and FF. In the ideal condition, J_{SC} is determined by the charge carrier density and charge carrier mobility, therefore the hole and electron mobility are important parameters for the total performance.[56] To investigate the effect of additive CN on the charge-carrier transport, the hole (μ_h) and the electron mobilities (μ_e) in the PTB7:PCPDT-PDI blends spin-coating from CF and CF:CN were measured by the space charge limited current (SCLC) method with the Mott–Gurney equation. The typical *J-V* curves of the hole-only and electron-only devices are shown in Fig. 6, which exhibit obvious Ohmic (slope = 1) and SCLC regions (slope = 2). The hole mobility of the films spin-coated from CF and CF:CN were estimated to be 1.0×10^{-4} and 1.3×10^{-4} cm^2 V^{-1} s^{-1}, respectively. The small changed hole mobility suggests that additive CN induces little effect

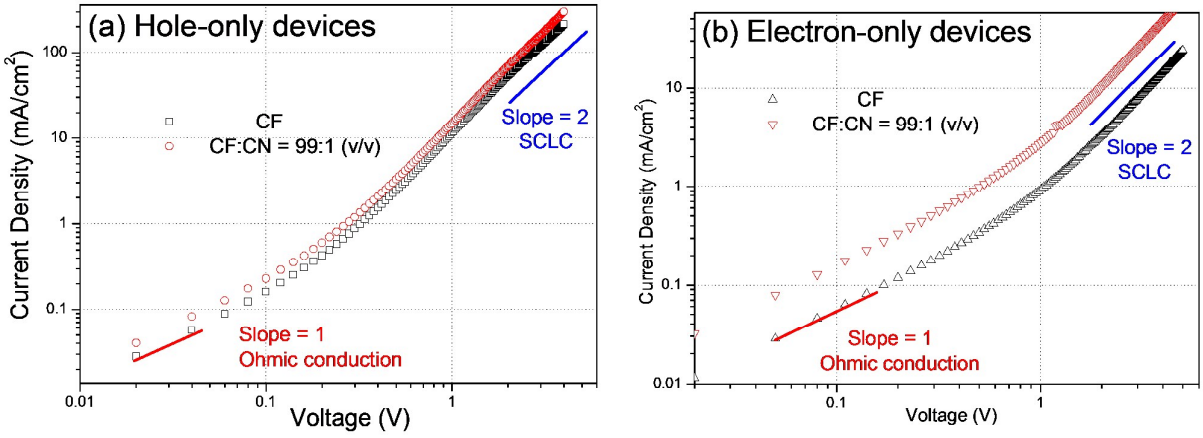

Fig. 6 Typical *J–V* curves based on **PTB7**:**PCPDT-PDI** composite for (a) the hole-only and (b) the electron-only devices spin-coated from CF and CF:CN=99:1 (v/v).

on the aggregation of PTB7 compared to the hole mobility of pure PTB7 reported as 2.5×10^{-4} cm^2 V^{-1} s^{-1}.[45] On the contrary, by adding 1.0 vol % of CN in CF, the electron mobility of the blend film improved from 2.8×10^{-6} cm^2 V^{-1} s^{-1} to 9.8×10^{-6} cm^2 V^{-1} s^{-1}, which might be caused by the aggregation of PCPDT-PDI and/or the purification of the n-type polymer domains. However, the μ_e/μ_h of 0.075 was still quite low, and this unbalanced charge mobility should be the reason of low fill factor and the consequent inferior photovoltaic performance, which implies there is still large development space for device with higher PCE.[20]

External quantum efficiency

Fig. 7 exhibits the external quantum efficiency (EQE) plots of polymer solar cells based on PTB7:PCPDT-NDI and PTB7:PCPDT-PDI films spin-coated from CF and CF:CN (99:1, v/v). PTB7:PCPDT-NDI device fabricated from CF shows the EQE peak value of 17%, which is slight larger than that of the device spin-coated from mixture solvent CF:CN. The decreasing EQE upon addition of CN might result from the lower efficient exciton diffusion due to the large aggregation domain. In contrast, the PTB7:PCPDT-PDI device spin-coated from CF:CN (99:1 v/v) has hegher EQE peak value of 34% than that of 23% obtained from the device fabricated from CF solvent. The increasing EQE in PTB7:PCPDT-PDI device upon addition of CN is in consistent with good phase separation and higher electron mobility, indicating that the additive CN not only improve the efficiency of exciton diffusion, but also enhance the charge carrier transport. Moreover, PTB7:PCPDT-PDI devices show higher EQE than that of PTB7:PCPDT-NDI in the wavelength region of 300-750 nm, however, the EQE of PTB7:PCPDT-NDI devices are higher than PTB7:PCPDT-PDI in the 750-950 nm region. From the UV-vis absorption, the larger EQE should mainly be attributed to the absorption of PCPDT-NDI.

Conclusions

In summary, two n-type copolymers PCPDT-NDI and PCPDT-PDI were synthesized by coupling planar CPDT unit with NDI and PDI moiety , respectively. Compared with PCPDT-PDI, PCPDT-NDI showed broader absorption spectrum and better crystallinity. The best photovoltaic performance for PTB7:PCPDT-NDI device is obtained by using CF as the solvent, and the addition of CN reduced the PCE due to the larger domain sizes. In contrast, PTB7:PCPDT-PDI device incorporating 1.0 v% CN as additive exhibited good film morphology and improved PCE of 2.13% with V_{OC} = 0.70 V, J_{SC} = 7.25 mA cm^{-2} and FF = 0.42. The occurrence of significantly increased J_{SC} might be due to the improved exciton dissociation into free charge carrier and enhanced electron mobility, proved by AFM and electron-only device measurements. The comparison of NDI and PDI-based n-type polymers could provide an insight toward optimum polymer for high performance all-polymer solar cells.

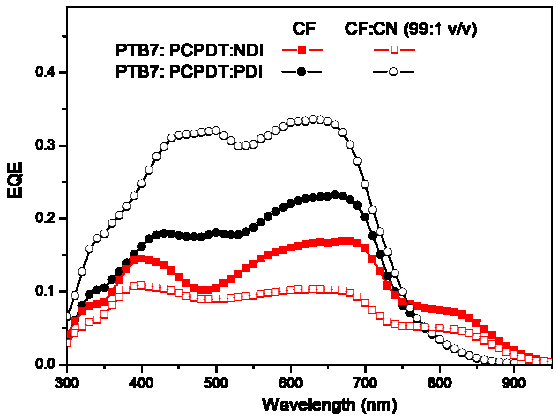

Fig. 7 External quantum efficiency (EQE) plots of polymer solar cells based on **PTB7**:**PCPDT-NDI** and **PTB7**:**PCPDT-PDI** films spin-coated from CF and CF:CN.

Acknowledgements

This work was supported by the National Natural Science Foundation (No. 51473040, 51203030).

Notes and references

1. E. Bundgaard and F. C. Krebs, *Sol. Energy Mater. Sol. Cells*., 2007, 91, 954-985.
2. H. J. Park, M. G. Kang, S. H. Ahn and L. J. Guo, *Adv. Mater.*, 2010, 22, E247-E253.
3. W. Cai, X. Gong and Y. Cao, *Sol. Energy Mater. Sol. Cells*., 2010, 94, 114-127.
4. R. Sondergaard, M. Hosel, D. Angmo, T. T. Larsen-Olsen and F. C. Krebs, *Mater. Today.*, 2012, 15, 36-49.
5. M. M. Mandoc, W. Veurman, L. J. A. Koster, B. de Boer and P. W. M. Blom, *Adv. Func. Mater.*, 2007, 17, 2167-2173.
6. K. D. Deshmukh, T. S. Qin, J. K. Gallaher, A. C. Y. Liu, E. Gann, K. O'Donnell, L. Thomsen, J. M. Hodgkiss, S. E. Watkins and C. R. McNeill, *Energy Environ. Sci.*, 2015, 8, 332-342.
7. Z. A. Tan, E. Zhou, X. Zhan, X. Wang, Y. Li, S. Barlow and S. R. Marder, *Appl. Phys. Lett.*, 2008, 93, 073309.
8. J. E. Anthony, A. Facchetti, M. Heeney, S. R. Marder and X. Zhan, *Adv. Mater.*, 2010, 22, 3876-3892.
9. J. R. Moore, S. Albert-Seifried, A. Rao, S. Massip, B. Watts, D. J. Morgan, R. H. Friend, C. R. McNeill and H. Sirringhaus, *Adv. Energy Mater.*, 2011, 1, 230-240.
10. L. M. Kozycz, D. Gao, A. J. Tilley and D. S. Seferos, *J. Polym. Sci., Part A: Polym. Chem.*, 2014, 52, 3337-3345.
11. S. Dai, P. Cheng, Y. Lin, Y. Wang, L. Ma, Q. Ling and X. Zhan, *Polym. Chem.*, 2015, 6, 5254-5263.
12. X. Zhan, Z. A. Tan, B. Domercq, Z. An, X. Zhang, S. Barlow, Y. Li, D. Zhu, B. Kippelen and S. R. Marder, *J. Am. Chem. Soc.*, 2007, 129, 7246-7247.
13. X. W. Zhan, Z. A. Tan, E. J. Zhou, Y. F. Li, R. Misra, A. Grant, B. Domercq, X. H. Zhang, Z. S. An, X. Zhang, S. Barlow, B. Kippelen and S. R. Marder, *J. Mater. Chem.*, 2009, 19, 5794-5803.
14. E. Zhou, J. Cong, Q. Wei, K. Tajima, C. Yang and K. Hashimoto, *Angew. Chem. Int. Ed.*, 2011, 50, 2799-2803.

15. P. Cheng, L. Ye, X. G. Zhao, J. H. Hou, Y. F. Li and X. W. Zhan, *Energy Environ. Sci.*, 2014, 7, 1351-1356.
16. Y. Zhou, Q. F. Yan, Y. Q. Zheng, J. Y. Wang, D. H. Zhao and J. Pei, *J. Mater. Chem. A*, 2013, 1, 6609-6613.
17. Y. Zhou, T. Kurosawa, W. Ma, Y. K. Guo, L. Fang, K. Vandewal, Y. Diao, C. G. Wang, Q. F. Yan, J. Reinspach, J. G. Mei, A. L. Appleton, G. I. Koleilat, Y. L. Gao, S. C. B. Mannsfeld, A. Salleo, H. Ade, D. H. Zhao and Z. N. Bao, *Adv. Mater.*, 2014, 26, 3767-3772.
18. H. Yan, Z. Chen, Y. Zheng, C. Newman, J. R. Quinn, F. Dotz, M. Kastler and A. Facchetti, *Nature*, 2009, 457, 679-686.
19. T. W. Holcombe, J. E. Norton, J. Rivnay, C. H. Woo, L. Goris, C. Piliego, G. Griffini, A. Sellinger, J. L. Bredas, A. Salleo and J. M. J. Frechet, *J. Am. Chem. Soc.*, 2011, 133, 12106-12114.
20. S. Fabiano, Z. Chen, S. Vahedi, A. Facchetti, B. Pignataro and M. A. Loi, *J. Mater. Chem.*, 2011, 21, 5891.
21. H. P. Yan, B. A. Collins, E. Gann, C. Wang, H. Ade and C. R. McNeill, *Acs Nano*, 2012, 6, 677-688.
22. M. Schubert, D. Dolfen, J. Frisch, S. Roland, R. Steyrleuthner, B. Stiller, Z. H. Chen, U. Scherf, N. Koch, A. Facchetti and D. Neher, *Adv. Energy Mater.*, 2012, 2, 369-380.
23. D. Mori, H. Benten, I. Okada, H. Ohkita and S. Ito, *Adv. Energy Mater.*, 2014, 4. 1301006.
24. J. Y. Yuan and W. L. Ma, *J. Mater. Chem. A*, 2015, 3, 7077-7085.
25. H. Kang, K. H. Kim, J. Choi, C. Lee and B. J. Kim, *Acs Macro. Lett.*, 2014, 3, 1009-1014.
26. H. Kang, M. A. Uddin, C. Lee, K. H. Kim, T. L. Nguyen, W. Lee, Y. Li, C. Wang, H. Y. Woo and B. J. Kim, *J. Am. Chem. Soc.*, 2015, 137, 2359-2365.
27. C. Mu, P. Liu, W. Ma, K. Jiang, J. B. Zhao, K. Zhang, Z. H. Chen, Z. H. Wei, Y. Yi, J. N. Wang, S. H. Yang, F. Huang, A. Facchetti, H. Ade and H. Yan, *Adv. Mater.*, 2014, 26, 7224-7230.
28. D. Mori, H. Benten, I. Okada, H. Ohkita and S. Ito, *Energy Environ. Sci.*, 2014, 7, 2939-2943.
29. E. Zhou, J. Cong, M. Zhao, L. Zhang, K. Hashimoto and K. Tajima, *Chem. Commun.,* 2012, 5283-5285.
30. E. Zhou, J. Z. Cong, K. Hashimoto and K. Tajima, *Adv. Mater.*, 2013, 25, 6991-6996.
31. T. Earmme, Y. J. Hwang, N. M. Murari, S. Subramaniyan and S. A. Jenekhe, *J. Am. Chem. Soc.*, 2013, 135, 14960-14963.
32. T. Earmme, Y.-J. Hwang, S. Subramaniyan and S. A. Jenekhe, *Adv. Mater.*, 2014, 26, 6080-6085.
33. C. Lee, H. Kang, W. Lee, T. Kim, K. H. Kim, H. Y. Woo, C. Wang and B. J. Kim, *Adv. Mater.*, 2015, 27, 2466-2471.
34. J. W. Jung, J. W. Jo, C.-C. Chueh, F. Liu, W. H. Jo, T. P. Russell and A. K. Y. Jen, *Adv. Mater.*, 2015, 27, 3310-3317.
35. Y.-J. Hwang, B. A. E. Courtright, A. S. Ferreira, S. H. Tolbert and S. A. Jenekhe, *Adv Mater*, 2015, 27, 4578-4584.
36. X. L. Hu, L. J. Zuo, H. B. Pan, F. Hao, J. Y. Pan, L. Fu, M. M. Shi and H. Z. Chen, *Sol. Energy Mater. Sol. Cells*., 2012, 103, 157-163.
37. S. Fabiano, S. Himmelberger, M. Drees, Z. H. Chen, R. M. Altamimi, A. Salleo, M. A. Loi and A. Facchetti, *Adv. Energy Mater.*, 2014, 4. 1301409.
38. M. Schubert, B. A. Collins, H. Mangold, I. A. Howard, W. Schindler, K. Vandewal, S. Roland, J. Behrends, F. Kraffert, R. Steyrleuthner, Z. H. Chen, K. Fostiropoulos, R. Bittl, A. Salleo, A. Facchetti, F. Laquai, H. W. Ade and D. Neher, *Adv. Funct. Mater.*, 2014, 24, 4068-4081.
39. J. Peet, J. Y. Kim, N. E. Coates, W. L. Ma, D. Moses, A. J. Heeger and G. C. Bazan, *Nat. Mater.*, 2007, 6, 497-500.
40. F. Etzold, I. A. Howard, N. Forler, D. M. Cho, M. Meister, H. Mangold, J. Shu, M. R. Hansen, K. Muellen and F. Laquai, *J. Am. Chem. Soc.*, 2012, 134, 10569-10583.
41. X. Liu, S. Huettner, Z. Rong, M. Sommer and R. H. Friend, *Adv. Mater.*, 2012, 24, 669-674.
42. L. Lu and L. Yu, *Adv. Mater.*, 2014, 26, 4413-4430.
43. S. Woo, W. H. Kim, H. Kim, Y. Yi, H.-K. Lyu and Y. Kim, *Adv. Energy. Mater.*, 2014, 4. 1301692.
44. F. Würthner, V. Stepanenko, Z. Chen, C. R. Saha-Möller, N. Kocher and D. Stalke, *J. Org. Chem.*, 2004, 69, 7933-7939.
45. Y. Liang, Z. Xu, J. Xia, S.-T. Tsai, Y. Wu, G. Li, C. Ray and L. Yu, *Adv. Mater.*, 2010, 22, E135-E138.
46. N. Zhou, H. Lin, S. J. Lou, X. Yu, P. Guo, E. F. Manley, S. Loser, P. Hartnett, H. Huang, M. R. Wasielewski, L. X. Chen, R. P. H. Chang, A. Facchetti and T. J. Marks, *Adv. Energy Mater.*, 2014, 4, 1300785.
47. E. Zhou, M. Nakano, S. Izawa, J. Cong, I. Osaka, K. Takimiya and K. Tajima, *ACS Macro. Lett.*, 2014, 3, 872-875.
48. D. Gendron and M. Leclerc, *Energy Environ. Sci.*, 2011, 4, 1225-1237.
49. T. Earmme, Y.-J. Hwang, N. M. Murari, S. Subramaniyan and S. A. Jenekhe, *J. Am. Chem. Soc.*, 2013, 135, 14960-14963.
50. J. H. Hou, S. Q. Zhang, T. L. Chen and Y. Yang, *Chem. Commun.,* 2008, 6034-6036.
51. J. L. Li, F. Dierschke, J. S. Wu, A. C. Grimsdale and K. Mullen, *J. Mater. Chem.*, 2006, 16, 96-100.
52. J. Huang, X. Wang, X. Zhang, Z. Niu, Z. Lu, B. Jiang, Y. Sun, C. Zhan and J. Yao, *Acs Appl. Mater. Inter.*, 2014, 6, 3853-3862.
53. M. S. Su, C. Y. Kuo, M. C. Yuan, U. S. Jeng, C. J. Su and K. H. Wei, *Adv. Mater.*, 2011, 23, 3315-3319.
54. Y.-W. Su, S.-C. Lan and K.-H. Wei, *Materials Today*, 2012, 15, 554-562.
55. S.-C. Lan, P.-A. Yang, M.-J. Zhu, C.-M. Yu, J.-M. Jiang and K.-H. Wei, *Polym. Chem.*, 2013, 4, 1132-1140.
56. S. Günes, H. Neugebauer and N. S. Sariciftci, *Chem. Rev.*, 2007, 107, 1324-1338.

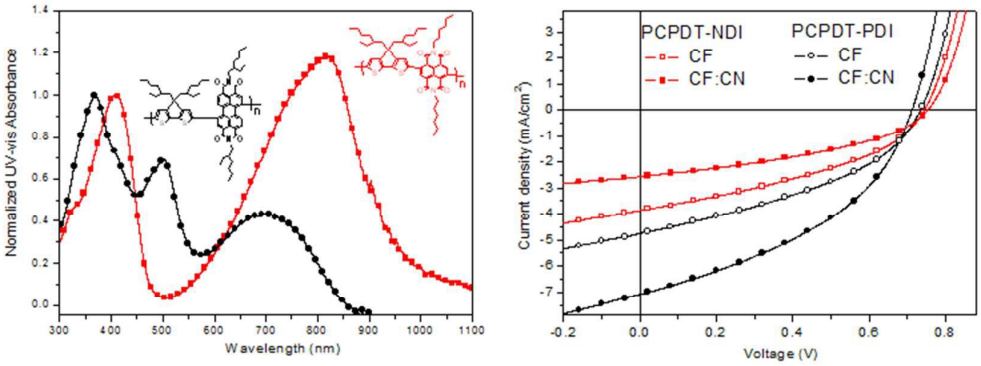

Two solution-processable clopenta[2,1-b:3,4-b']dithiophene (CPDT)-based n-type copolymers, PCPDT-NDI and PCPDT-PDI were synthesized. Although PCPDT-NDI has better near-infrared (850-1100 nm) light harvesting and crystalline properties, the PCE is as low as 1.12% mainly due to poor miscibility and film quality. PCPDT-PDI device exhibits much better efficiency with PCE of 2.13% by using 1-chloronaphthalene (CN) as additive to improve the electron mobility.